EUROPEAN ORGANIZATION FOR NUCLEAR RESEARCH

L3 Note **2550**
22 June, 2000

Search for Exotic Unstable Heavy Leptons in e^+e^- Annihilation at $\sqrt{s} = 192 - 202$ GeV

The L3 Collaboration

Abstract

A search for exotic unstable heavy leptons (sequential, vector, mirror and singlet leptons) is made at center-of-mass energies $\sqrt{s} = 192{-}202$ GeV with the L3 detector at LEP. No evidence for their existence is found. For pair-produced heavy leptons lower limits on their masses are set. For singly-produced heavy neutrino we set upper limits on the mixing parameter between the heavy and light neutrinos.

Submitted to the *XXXth International Conference on High Energy Physics*
July 27 - August 2, 2000, Osaka, Japan

Introduction

Many theories beyond the Standard Model (SM) predict the existence of new heavy leptons [1]. The predicted production cross sections are large and final state particles can be identified cleanly. Results on this subject (mainly search for new sequential leptons) obtained at the Z resonance by LEP and SLC experiments can be found in [2], and more recent results obtained at LEP at $\sqrt{s} = 133-189$ GeV can be found in [3]. Here we report on a direct search for exotic unstable heavy leptons. The data used in this analysis were collected with the L3 detector at LEP during 1999 at $\sqrt{s} = 192-202$ GeV with total integrated luminosity 233 pb^{-1}. We have combined the results with our earlier data recorded at $\sqrt{s} = 133-189$ GeV. The L3 detector is described elsewhere [4].

The exotic leptons discussed in this paper may be classified by $SU(2) \times U(1)$ quantum numbers [1]:

i) Sequential leptons: they exist in the simplest extension of the SM where one simply adds to the known fermionic spectrum a fourth family with the same quantum numbers. The indirect limits on existence of these particles coming from studies of electroweak precision data can be found in [5].

ii) Vector leptons: for these particles both left-handed and right-handed components are in weak isodoublets. For example, they are predicted in the E_6 group [6].

iii) Mirror leptons [7]: these particles have chiral properties which are opposite to those of ordinary leptons, i.e. right-handed components are in weak isodoublets and left-handed ones are in weak isosinglets. Mirror fermions appear in many extensions of th SM and provide a possble way to restore left-right symmetry at the scale of the electroweak symmetry breaking.

iv) Singlet neutrinos: these particles are the most discussed fermions in the literature. They arise in many models such as Grand Unified Theories, Superstring inspired models, left-right symmetric and see-saw models [8]

Production and decay of exotic leptons

Sequential, vector and mirror heavy leptons are pair-produced through the s-channel via γ and Z boson exchange for charged leptons ($\mathrm{L}^+\mathrm{L}^-$), while for heavy neutrinos ($\mathrm{L}^0\overline{\mathrm{L}}^0$) only Z boson exchange is present. The total cross sections are in the range of 1–3 pb at masses well below the beam energy and fall as the mass of the lepton approaches the beam energy (see Figures 1 and 2). The neutral heavy leptons could be either of Dirac or Majorana types. The main difference between pair-produced Dirac and Majorana neutrinos is the dependence of the cross section on velocity $\beta = \mathrm{P_L}/\sqrt{\mathrm{P_L^2} + \mathrm{m_L^2}}$: $\sigma_{Dirac} \propto \beta(3-\beta^2)$ and $\sigma_{Majorana} \propto \beta^3$. Due to the β^3 term the cross section for Majorana neutrinos falls more rapidly with mass than the cross section for Dirac neutrinos. In this search we consider that heavy leptons couple to electron, muon, or tau families and we neglect the possibility of mixing between light leptons.

The mixing between the isosinglet neutrino and its associated isodoublet neutrino allows single production to occur in $\mathrm{e}^+\mathrm{e}^-$ annihilation:

$$\mathrm{e}^+\mathrm{e}^- \rightarrow \mathrm{N}_\ell + \nu_\ell.$$

One isosinglet neutrino N_ℓ is assumed to be associated with each generation of light neutrinos via the mixing amplitude U_ℓ. We do not consider mixing of the light neutrinos with higher isodoublet states (sequential leptons) nor the possibility of mixing among light neutrinos (as discussed in Ref. [9]). In contrast to sequential, vector and mirror neutral leptons where pair production is dominant (when kinematically allowed), here single production dominates. The corresponding pair production cross section is suppressed relatively to the single production cross section by an additional $|U_\ell|^2$ factor, which is expected to be small (from indirect searches at LEP1 and low-energy experiments $|U_\ell| \leq 0.1$ for m_{N} larger than 80 GeV [10]). The single production process proceeds through s-channel Z exchange for all generations. For the first generation, $\mathrm{N_e}$, when heavy neutrinos can couple to electrons, there is an additional contribution from t-channel W exchange (see Figure 3). Due to this additional contribution the production cross section for the first generation heavy neutrinos can be as high as 0.6 pb for mixing amplitude $|U_\ell| = 0.1$ (see Figure 4). Since the mixing amplitude is expected to be small, the production cross section for N_μ and N_τ is too small to be explored at LEP2. Therefore, in this paper we concentrate on the search for the first generation heavy singlet neutrino, $\mathrm{N_e}$.

Exotic heavy leptons decay via the charged or neutral weak currents through the mixing with a light lepton, except for sequential heavy leptons, which decay only through charged current (the existence of non-diagonal neutral currents is forbidden in the SM as a result of the GIM mechanism [11]):

$$\mathrm{L}^- \to \nu_\ell W \text{ or } \mathrm{L}^- \to \ell Z$$

$$\mathrm{L}^0 \to \ell W \text{ or } \mathrm{L}^0 \to \nu_\ell Z$$

$$\mathrm{N_e} \to \mathrm{eW} \text{ or } \mathrm{N_e} \to \nu_\mathrm{e}\mathrm{Z},$$

where $\ell = e, \mu, \tau$. For heavy lepton masses not far above the W mass, heavy neutrinos decay predominantly through the W boson due to phase space suppression of the decay into Z, while for large masses $Br(\mathrm{N_e} \to \mathrm{eW}) = 0.67$ and $Br(\mathrm{N_e} \to \nu_\mathrm{e}\mathrm{Z}) = 0.33$ [12](see Figure 5). In this paper we consider only the decay into W boson.

If the decay proceeds via mixing, the decay amplitude contains a mixing parameter U for the transition from the heavy lepton to the light lepton. The mean decay length, D, as a function of $|U|^2$ and mass is given by [9] $\mathrm{D} = \beta\gamma c\tau_\mathrm{L} \propto \beta |U|^{-2} m_\mathrm{L}^\alpha$, where τ_L is the lifetime of the heavy lepton and $\alpha \approx -6$. This implies that the decay can occur far from the interaction point if the particle has a low mass or a very small coupling. To ensure high detection and reconstruction efficiencies, the search is restricted to L^0's decaying within 1 cm of the interaction point. This limits the sensitivity to the mixing parameter to $|U|^2 > \mathcal{O}(10^{-11})$.

Event Simulation

The generation of pair-produced heavy lepton and decay is done with the TIPTOP [13] Monte-Carlo program. It incorporates initial state radiative corrections, the spin effects on the decay distribution and the effects of the finite width of the produced W bosons. For pair production of heavy leptons we consider the mass range between 50 and 100 GeV. Using the full differential cross section [14], a dedicated Monte Carlo generator is constructed to simulate heavy singlet neutrino production and decay. Subsequent hadronic fragmentation and decay are simulated by the JETSET Monte Carlo program [15]. Initial and final state radiation is taken into account. In addition, we include the effects of the finite width of the produced W and Z bosons. For single production of heavy neutrino we consider the mass range between 80 and 195 GeV.

For the simulation of background from Standard Model processes the following Monte Carlo programs were used: PYTHIA 5.7 [16] ($e^+e^- \to q\bar{q}(\gamma)$, Ze^+e^-, ZZ, $W^\pm e^\mp \nu$), KORALZ [17] ($e^+e^- \to \tau^+\tau^-(\gamma)$), KORALW [18] ($e^+e^- \to W^+W^-$), PHOJET [19] ($e^+e^- \to e^+e^- q\bar{q}$), DIAG36 [20] ($e^+e^- \to e^+e^-\tau^+\tau^-$), and EXCALIBUR [21] ($e^+e^- \to f\bar{f}'f\bar{f}'$).

The Monte-Carlo events have been simulated in the L3 detector using the GEANT3 program [22], which takes into account the effects of energy loss, multiple scattering and showering in the materials.

Lepton and Jet Identification, and Background Rejection

An electron is identified as a cluster in the electromagnetic calorimeter with an energy larger than 4 GeV matched to a track in the (R, ϕ) plane to within 20 mrad. The cluster profile should be consistent with the one expected for an electron, *i.e.* we require $0.95 < E_9/E_{25} < 1.05$, where $E_{9(25)}$ is the corrected sum of energies of 9(25) BGO crystals around the most energetic one (including the energy of the most energetic one). The electron candidate must have $|\cos\theta| < 0.94$. Muons are measured by the muon chamber system surrounding the calorimeters. We require that a muon track consists of track segments in at least two layers of muon chambers, and that the muon track points back to the interaction region. The muon momentum must be greater than 4 GeV and it must be in the fiducial volume defined by $|\cos\theta| < 0.8$. In the following analysis lepton isolation is also required. The lepton is isolated if the energy in a 30° cone around it, is smaller than 5 GeV. Moreover, for isolated electrons we require only one matched track to eliminate converted photons. Jets are reconstructed from electromagnetic and hadronic calorimeter clusters using the Durham algorithm [23] with a jet resolution parameter of $y_{cut} = 0.008$. The jet momenta are defined by the vectorial energy sum of calorimetric clusters.

The most important backgrounds for the new heavy lepton searches are W^+W^-, $q\bar{q}(\gamma)$ and ZZ production for the signatures with large visible energy and two-photon processes for the signatures with small visible energy. The two-photon and $q\bar{q}(\gamma)$ processes can be rejected demanding transverse momentum imbalance, the absence of energy in the very forward-backward regions, and a missing momentum vector not pointing to the very forward-backward regions. The cut on the number of hadronic jets in the event is also important. For W^+W^- process rejection, a variety of cuts on visible mass, number of hadronic jets, jet angles and energies, lepton energies, invariant mass of the lepton and unseen neutrino could be used. For ZZ process rejection a cut on the energy sum of the two isolated leptons could be used.

Search for pair-produced exotic leptons

Search for pair-produced neutral leptons

The event topology used in the search is two isolated leptons (e, μ, or τ) of the same family plus the decay products of real or virtual W bosons, i.e. $e^+e^- \to L^0\bar{L}^0 \to \ell^+\ell^- W^{+*}W^{-*}$. Hadronic events with visible energy greater than 60 GeV and charged track multiplicity greater than 3 are used in this analysis.

For the case where both neutral heavy leptons decay to either electrons or muons, events must also satisfy the following criteria:

- The number of reconstructed jets plus isolated leptons is at least 3.
- The energy sum of the two isolated electrons or muons must be less than 70 GeV. This is a cut introduced to reject the Z-pair background. Figure 6 shows an example of the isolation criteria.

Table 1: The number of selected events and expected background for pair-produced unstable neutral heavy lepton L^0.

Decay mode	$\sqrt{s}$	Data	Background
$L^0 \to eW$	192 GeV	0	0.6
	196 GeV	3	1.7
	200 GeV	2	1.7
	202 GeV	1	0.8
	Total	5	4.8
$L^0 \to \mu W$	192 GeV	0	0.2
	196 GeV	1	0.5
	200 GeV	2	0.5
	202 GeV	0	0.2
	Total	3	1.4
$L^0 \to \tau W$	192 GeV	4	7.4
	196 GeV	25	21.9
	200 GeV	20	26.0
	202 GeV	8	10.9
	Total	57	66.2

For the case where both neutral heavy leptons decay to tau leptons, each of the taus can independently decay to hadrons, muons, or electrons. When both tau leptons decay to either muons or electrons, the above selection is applied with the exception that we allow the isolated leptons to be either two electrons, two muons, or one muon and one electron. We also consider the final state in which at least one of the tau decays into one charged hadron. In this case, events satisfying the following criteria are selected:

- The number of reconstructed jets plus isolated leptons is at least 4.
- The polar angle (angle with the beam axis) θ of the missing momentum must be in the range $25° < \theta < 155°$, and the fraction of visible energy in the forward-backward region ($\theta < 20°$ and $\theta > 160°$) must be less than 40%.
- The angle between the most isolated track and the track nearest to it, must be greater than 50° or the angle between the second most isolated track and the track nearest to it, must be greater than 25°. The transverse momenta, p_t, of the two most isolated tracks must be greater than 1.2 GeV, and at least one track must have p_t greater than 2.5 GeV.
- The electron and muon energies must be less than 50 GeV.

Table 1 shows the number of selected events and expected SM background for electron, muon and tau decay modes.

Search for pair-produced charged leptons

For this search, two sets of cuts are used to search for the topology with one hadronic and one leptonic W-decay as well as two hadronic W-decays. For both selections we require that the visible energy be greater than 50 GeV, the multiplicity of charged tracks be greater than 3, and the fraction of the total visible energy in the forward-backward region be less than 25%.

For the mode $\mathrm{L}^+\mathrm{L}^- \to \nu_\ell\bar{\nu}_\ell\ \mathrm{W}^{+*}\mathrm{W}^{-*} \to \nu_\ell\bar{\nu}_\ell\ell\nu_\ell q\bar{q}'$, events satisfying the following criteria are selected:

- The event contains at least one isolated electron or muon with energy greater than 15 GeV and less than 60 GeV.
- The number of reconstructed jets plus isolated leptons is at least 3.
- The polar angle θ of the missing momentum must be in the range $25° < \theta < 155°$.
- The sum of the energies of the hadronic jets must be less than $\sqrt{s}/2-12.5$ GeV. Figure 7 shows the distribution of the sum of the energies of hadronic jets, after all other cuts have been applied.

For the mode where both W bosons decay hadronically, events satisfying the following criteria are selected:

- The event does not contain any isolated electrons or muons and the energy of each non-isolated electron or muon must be less than 30 GeV.
- The number of hadronic jets is at least 4.

For charged heavy lepton masses greater than the W boson mass, the leptons each decay to a real W. The dominant remaining background after the previous cuts have been applied is W-pair production. However, for the signal events, due to the energy and momentum carried away by light neutrinos, the total visible energy is less than $\sqrt{s}$ and the two W bosons are not back-to-back. To improve the determination of jet energies and angles (both for the signal and the background) a kinematic fit is applied imposing the constraint that both jet-jet invariant masses are equal to the W mass. All possible jet-jet combinations are considered and the one which gives the smallest χ^2 of the fit is chosen. The following additional requirements are then imposed for the case where the charged lepton mass is greater than 80 GeV:

- The visible energy must be less than $\sqrt{s} - 20$ GeV. Figure 8 shows the distribution of visible energy, after all previous cuts have been applied.
- The acollinearity angle between the two W candidates is greater than 20°. Figure 9 shows the acollinearity angle distribution, after all previous cuts have been applied.
- The total transverse momentum of jets must be greater than 10 GeV. Figure 10 shows the distribution of this quantity, after all other cuts have been applied.

Table 2 shows the number of selected events and expected SM background.

Table 2: The number of selected events and expected background for pair-produced unstable charged heavy lepton $L^{\pm}$.

Decay mode	$\sqrt{s}$	Data	Background
$L^{\pm} \to \nu W^{\pm}$	192 GeV	11	8.1
	196 GeV	31	29.2
	200 GeV	25	30.5
	202 GeV	10	14.0
	Total	77	81.8

Search for singly-produced heavy neutrino

The most important backgrounds for heavy neutrino searches are W^+W^-production with one hadronic and one leptonic W decay (92% of the background), $q\bar{q}(\gamma)$ (6%) and ZZ production (2%). Reducing the W^+W^- background requires full reconstruction of the heavy neutrino mass from its decay products. The only decay channel for which this is possible is $N_e \to eW$ with $W \to$ jets. Thus, the event signature is one isolated electron [1)] plus hadronic jets. This channel has the largest branching ratio varying between 68% and 45% depending on the heavy neutrino mass.

The event selection requires at least two hadronic jets plus one isolated electron. The visible energy must be greater than 70 GeV and the number of reconstructed tracks must be greater than 6. The polar angle θ of the missing momentum should be in the range $25^\circ < \theta < 155^\circ$. The visible invariant mass m_{vis} of the event is reconstructed and, to improve the resolution, it is rescaled according to

$$m_{\mathrm{N}} = m_{vis} \frac{\sqrt{s}}{p_\nu + E} \ ,$$

where p_ν is the missing momentum of the event, and E is the visible energy. Figure 11 shows the rescaled invariant mass m_{N} of the events after all previous cuts have been applied. Two regions are defined. In region 1, where the heavy neutrino mass is close to the W mass, a significant fraction of W's produced in N_e decays are off-shell. In region 2, $m_{\mathrm{N}} > 100$ GeV, the W's are produced on-shell. In this case to further improve the resolution on the mass measurement, the determination of jet energies and angles, and the missing momentum direction (both for the signal and the W^+W^- background), a kinematic fit is applied imposing four-momentum conservation and the constraint that the invariant mass of the hadronic jets is equal to the W mass. In total, 15 events are selected in region 1, while 13.5 are expected from the background. The corresponding numbers for region 2 are 405 and 391.2. Figure 12 shows the distribution of the invariant mass of the electron and missing momentum, $m_{e\nu}$, for events in region 2 after the kinematic fit has been applied. One can see a clear peak at 80 GeV coming from the W^+W^- background.

The final selection requires the invariant mass of the electron and missing momentum to be outside the W mass region. Applying the cut, $m_{e\nu} < 70$ GeV or $m_{e\nu} > 90$ GeV, rejects 82% of the background events. Figure 13 shows the invariant mass of the events accepted after the

[1)] In this analysis the lepton is isolated if the energy in a 10° cone around it, is smaller than 5 GeV.

mass cut is applied. We observe a good agreement between data and expected background: 110 events pass the selection, while 98.1 are expected from the SM background.

Results

We see no signal. The number of selected events and expected background are in good agreement (see Tables 1 and 2, Figure 13). We calculate the 95% confidence level limits following the procedure in reference [24]. The systematic error, which is mainly due to the uncertainties in the energy calibration factors, the lepton identification efficiency and purity, and Monte Carlo statistics, is estimated to be 5% relative. To obtain exclusion limits, the selection efficiency has been reduced by one standard deviation in the total systematic error. We have combined the results with our earlier data recorded at $\sqrt{s} = 133 - 189$ GeV.

The selection efficiencies are determined by Monte-Carlo. For pair-produced neutral heavy leptons in the vicinity of the mass limit from 85 to 98 GeV, it is 23.3% to 39.0% for the electron decay mode. For the muon decay mode the efficiency in the same mass range is 27.0% to 33.3% . For the tau decay mode, the selection efficiency ranges from 23.0% for 75 GeV to 12.5% for 90 GeV. The selection efficiency for 98 GeV charged heavy lepton is 23.5%. Taking into account the luminosities, the selection efficiencies and the production cross section we obtain a lower limit on the mass of pair-produced heavy leptons (see Tables 3 and 4). The limits for vector heavy leptons are higher than for sequential and mirror ones due to the fact that the production cross section for vector leptons is larger.

Table 3: 95% CL lower mass limits (in GeV/c^2) for pair-produced neutral heavy leptons.

Decay mode	Model	Dirac	Majorana
$L^0 \to e$W	Sequential	97.1	85.7
	Vector	99.5	–
	Mirror	96.9	85.7
$L^0 \to \mu$W	Sequential	97.0	88.0
	Vector	99.4	–
	Mirror	96.7	88.0
$L^0 \to \tau$W	Sequential	89.0	79.6
	Vector	96.0	–
	Mirror	89.0	79.6

Table 4: 95% CL lower mass limits (in GeV/c^2) for pair-produced charged heavy leptons.

Decay mode	Model	
$L^0 \to \nu$W	Sequential	98.8
	Vector	99.1
	Mirror	98.7

For singlet heavy neutrino we calculate the 95% confidence level upper limit on the square of the mixing amplitude, $|U_{\mathrm{e}}|^2$. In region 1 we use the total number of events found in data and MC background to set a limit. In region 2 the number of events in data and MC background for a given mass m_{N} is defined as the number of events which have a reconstructed mass in the range of $m_{\mathrm{N}} \pm 2\sigma$, where mass resolution σ varies from 2 to 2.5 GeV over the mass range considered. The selection efficiency varies from 20% to 45% depending on the heavy neutrino mass and the center-of-mass energy. The results for the mixing amplitude, $|U_{\mathrm{e}}|^2$, as a function of the mass are shown in Figure 14. These limits are the only results for masses of singlet heavy neutrinos greater than 80 GeV.

Acknowledgements

I'm grateful to Marat Gataullin, the author of the Monte Carlo generator to simulate heavy singlet neutrino production and decay, for providing me with heavy neutrino generated samples and for preparing Figures 3-5.

References

[1] For a review see:
Exotic Fermions D. London, in *Precision Tests of the Standard Model*, ed. P. Langacker, Singapore, World Scientific (1995);
New Particles and Interactions A. Djouadi, J. Ng and T.G. Rizzo, in *Electroweak Symmetry Breaking and New Physics at the TeV Scale*, ed. T. Barklow, S. Dawson, H.E. Habor and S. Siegrist, Singapore, World Scientific (1997).

[2] ALEPH Collaboration, D. Decamp *et al.*, Phys. Lett. **B 236** (1990) 511;
ALEPH Collaboration, D. Decamp *et al.*, Phys. Rep. **216** (1992) 253;
DELPHI Collaboration, P. Abreu *et al.*, Nucl. Phys. **B 367** (1991) 511;
DELPHI Collaboration, P. Abreu *et al.*, Phys. Lett. **B 274** (1992) 230;
DELPHI Collaboration, P. Abreu *et al.*, Z. Phys. **C 74** (1997) 57:
L3 Collaboration, B. Adeva *et al.*, Phys. Lett. **B 251** (1990) 321;
L3 Collaboration, O. Adriani *et al.*, Phys. Lett. **B 295** (1992) 371;
L3 Collaboration, O. Adriani *et al.*, Phys. Rep. **236** (1993) 1;
OPAL Collaboration, M.Z. Akrawy *et al.*, Phys. Lett. **B 240** (1990) 250;
OPAL Collaboration, M.Z. Akrawy *et al.*, Phys. Lett. **B 247** (1990) 448;
OPAL Collaboration, M.Z. Akrawy *et al.*, Phys. Lett. **B 252** (1990) 290;
OPAL Collaboration, G. Alexander *et al.*, Z. Phys. **C 52** (1991) 200;
MARK II Collaboration, G.S. Abrams *et al.*, Phys. Rev. Lett. **63** (1989) 2447;
MARK II Collaboration, G.K. Jung *et al.*, Phys. Rev. Lett. **64** (1990) 1091;
MARK II Collaboration, P.R. Burchat *et al.*, Phys. Rev. **D 41** (1990) 3542;
MARK II Collaboration, E. Soderstrom *et al.*, Phys. Rev. Lett. **64** (1990) 2980.

[3] ALEPH Collaboration, D. Buskulic *et al.*, Phys. Lett. **B 384** (1996) 439;
ALEPH Collaboration, R. Barate *et al.*, Phys. Lett. **B 405** (1997) 379;
DELPHI Collaboration, P. Abreu *et al.*, Phys. Lett. **B 396** (1997) 315;
DELPHI Collaboration, P. Abreu *et al.*, Phys. Lett. **B444** (1998) 491;
DELPHI Collaboration, P. Abreu *et al.*, E. Phys. J. **C8** (1999) 41;
L3 Collaboration, M. Acciarri *et al.*, Phys. Lett. **B 377** (1996) 304;
L3 Collaboration, M. Acciarri *et al.*, Phys. Lett. **B 412** (1997) 189;
L3 Collaboration, M. Acciarri *et al.*, Phys. Lett. **B 461** (1999) 397;
L3 Collaboration, M. Acciarri *et al.*, Phys. Lett. **B 462** (1999) 354;
OPAL Collaboration, G. Alexander *et al.*, Phys. Lett. **B 385** (1996) 433;
OPAL Collaboration, K. Ackerstaff *et al.*, Phys. Lett. **B 393** (1997) 217;
OPAL Collaboration, K. Ackerstaff *et al.*, Eur. Phys. J. **C 1** (1998) 45;
OPAL Collaboration, K. Ackerstaff *et al.*, Phys. Lett. **B 433** (1998) 195;
OPAL Collaboration, K. Ackerstaff *et al.*, Preprint CERN-EP/99-169 to be published in Eur. Phys. J. **C**.

[4] L3 Collaboration, B. Adeva *et al.*, Nucl. Instr. Meth. **A 289** (1990) 35;
M. Acciari *et al.*, Nucl. Instr. Meth. **A 351** (1994) 300;
M. Chemarin *et al.*, Nucl. Instr. Meth. **A 349** (1994) 345;
M. Adam *et al.*, Nucl. Instr. Meth. **A 383** (1996) 342;
G. Basti *et al.*, Nucl. Instr. Meth. **A 374** (1996) 293.

[5] N. Evans, Phys. Lett. **B 340** (1994) 81;
P. Bamert and C.P. Burgess, Z. Phys. **C 66** (1995) 495;
T. Inami *et al.*, Mod. Phys. Lett. **A 10** (1995) 1471;
A. Masiero *et al.*, Phys. Lett. **B 355** (1995) 329;
V. A. Novikov, L.B. Okun, A.N. Rozanov *et al.*, Mod. Phys. Lett. **A 10** (1995) 1915; Erratum - ibid. **A 11** (1996) 698;
J. Erler, P. Langaster, Review of Particle Physics, Eur. Phys. J. **C 3** (1998) 91, Chapter 10.6;
M. Maltoni, V. A. Novikov, L.B. Okun *et al.*, hep-ph/9911535 (1999).

[6] For a review, see J. Hewett and T.G. Rizzo, Phys. Rep. **183**, 193 (1989).

[7] M. Maalampi and M. Roos, Phys. Rep. **186** 53 (1990).

[8] For a review, see J.W.F. Valle, Nucl. Phys. (Proc. Suppl) **11** (1989) p.118. M. Gell-Mann, P. Ramond, R. Slansky in Supergravity, eds. by D. Freedman *et al.*, (North Holland, 1979);
T. Yanagida, KEK lectures, eds. O. Sawada *et al.* (1979);
R. Mohaparta, G. Senjanovic, Phys. Rev. Lett. **44** (1980) 912, Phys. Rev. **D23** (1981) 165.

[9] M. Gronau, C. Leung and J. Rosner, Phys. Rev. **D 29** (1984) 2539.

[10] E. Nardi, E. Roulet and D. Tommasini, Phys. Lett. **B 344** (1995) 225;
New Particles and Interactions A. Djouadi, J. Ng and T.G. Rizzo, in *Electroweak Symmetry Breaking and New Physics at the TeV Scale*, ed. T. Barklow, S. Dawson, H.E. Habor and S. Siegrist, Singapore, World Scientific (1997).

[11] S.L. Glashow, J. Iliopoulos and L. Maiani, Phys. Rev. **D 2** (1970) 1285.

[12] A. Djouadi, Z. Phys. **C 63** (1994) 317;
G. Azuelos and A. Djouadi, Z. Phys. **C 63** (1994) 327.

[13] S. Jadach and J. Kühn, TIPTOP Monte Carlo, Preprint MPI-PAE/PTh 64/86.

[14] W. Buchmüller and C. Greub, Nucl. Phys. **B 363** (1991) 345.

[15] T. Sjöstrand, Comp. Phys. Comm. **82** (1994) 74.

[16] PYTHIA Monte Carlo Program: T. Sjöstrand, Comp. Phys. Comm. **82** (1994) 74.

[17] S. Jadach, J. Kühn and Z. Was, Comp. Phys. Comm. **64** (1991) 275;
S. Jadach, B.F.L.Ward and Z. Was, Comp. Phys. Comm. **66** (1991) 367.

[18] Monte Carlo program KORALW 1.02;
M. Skrzypek, S.Jadach, W. Placzek and Z. Was, CERN preprint CERN-TH/95-205, to be published in Comp. Phys. Comm.

[19] R. Engel, Z. Phys. **C 66** (1993) 1657.

[20] F.A. Berends, P.H. Daverveldt and R. Kleiss, Nucl. Phys. **B 253** (1985) 421; Comp. Phys. Comm. **40** (1986) 271.

[21] F.A. Berends, R. Kleiss and R. Pittau, Nucl. Phys. **B424** (1994) 308; Nucl. Phys. **B426** (1994) 344; Nucl. Phys. (Proc. Suppl.) **B37** (1994) 163; Phys. Lett. **B 335** (1994) 490; R. Kleiss and R. Pittau, Comp. Phys. Comm. **83** (1994) 141.

[22] The L3 detector simulation is based on GEANT Version 3.15. See R. Brun et al., "GEANT 3", CERN DD/EE/84-1 (Revised), September 1987. The GHEISHA program (H. Fesefeldt, RWTH Aachen Report PITHA 85/02 (1985)) is used to simulate hadronic interactions.

[23] Y.L. Dokshitzer, Contribution to the Workshop on Jets at LEP and HERA, Durham (1990);
N. Brown and W.J. Stirling, Rutherford Preprint RAL-91-049;
S. Catani *et al.*, Phys. Lett. **B 269** (1991) 432;
S. Bethke *et al.*, Nucl. Phys. **B 370** (1992) 310.

[24] V.F. Obraztsov, Nucl. Inst. Meth. **A 316** (1992) 388.

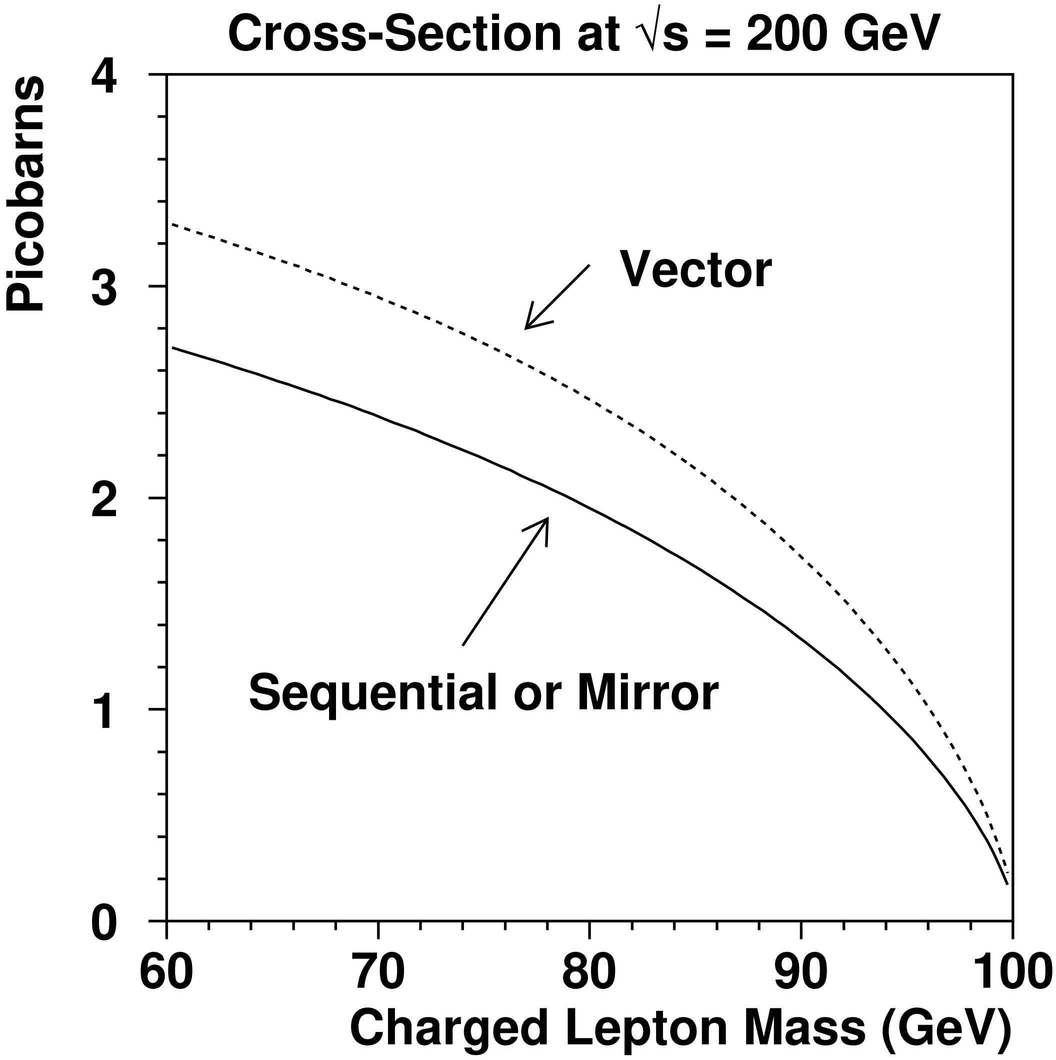

Figure 1: Total cross section for pair production of charged exotic leptons.

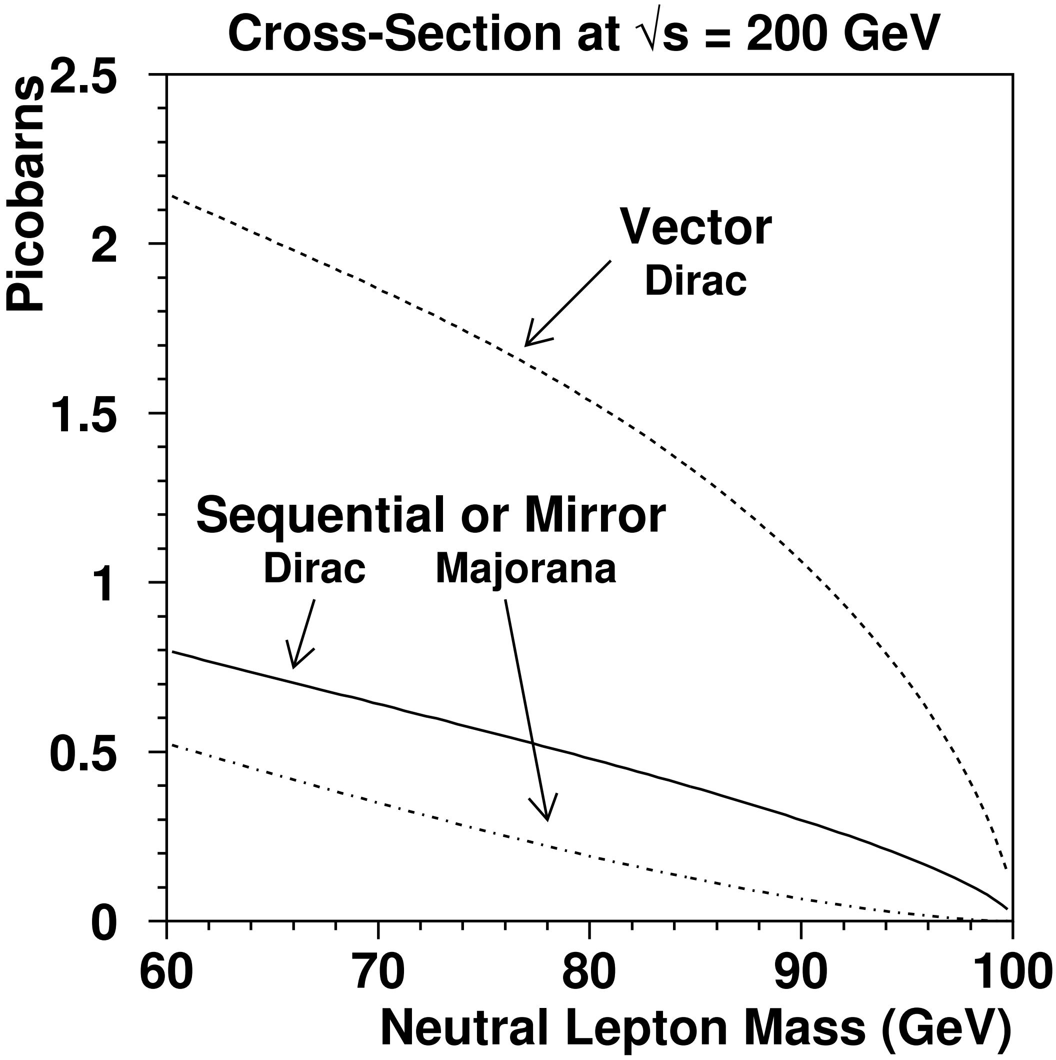

Figure 2: Total cross section for pair production of neutral exotic leptons.

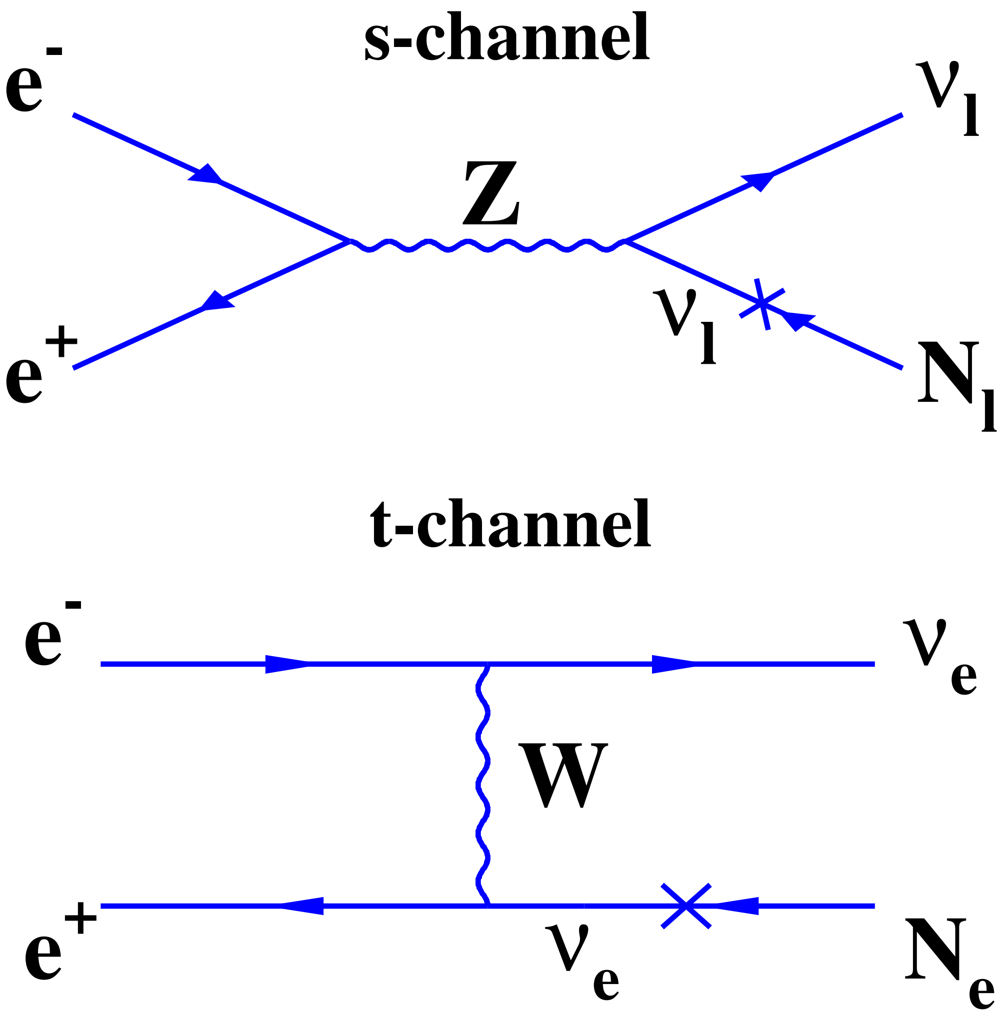

Figure 3: Feynman diagrams showing the production of isosinglet heavy neutrinos. Here the lepton ℓ denotes e, μ, or τ for s-channel production.

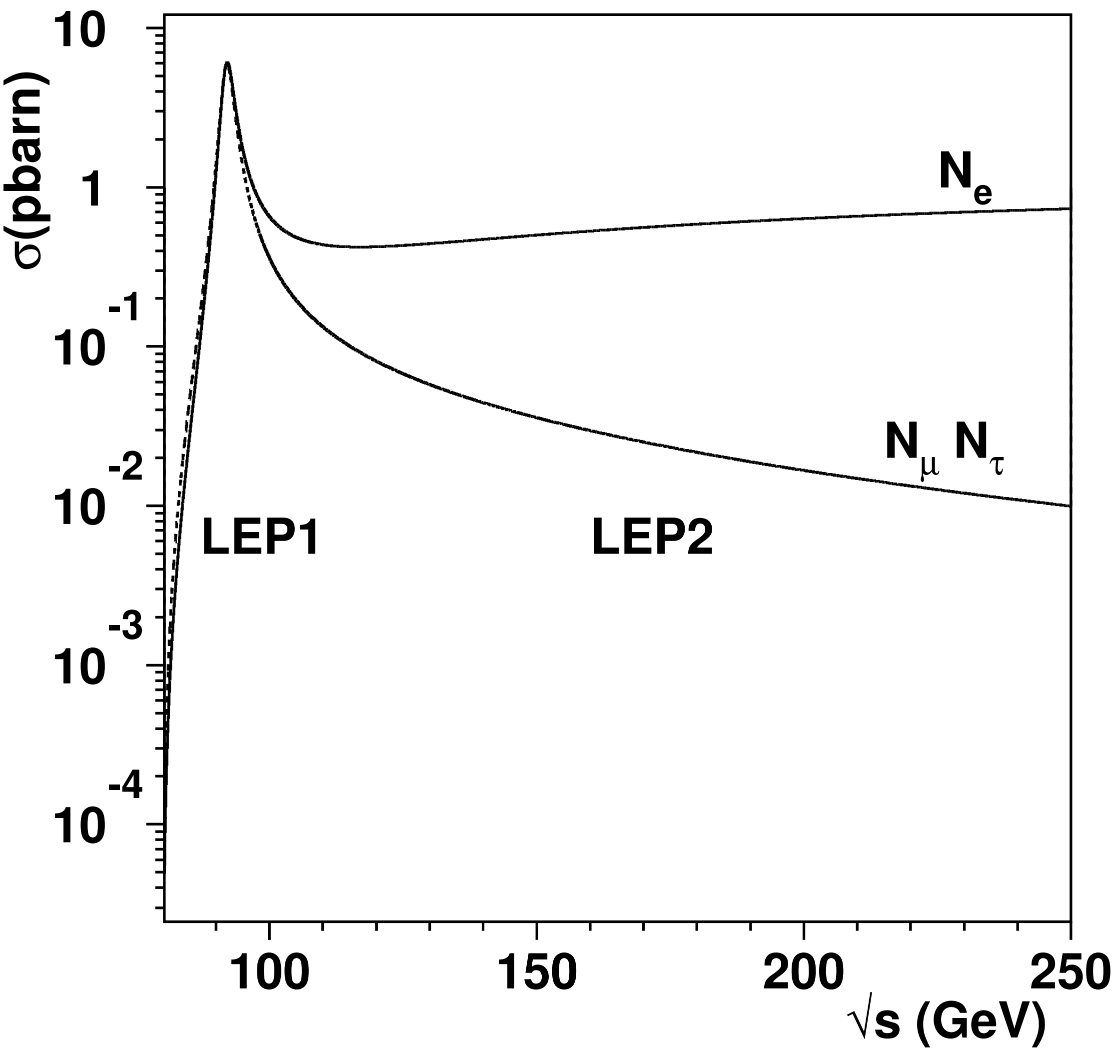

Figure 4: Total cross section for single production of singlet heavy neutrinos, $e^+e^- \to \mathrm{N}_\ell \nu_\ell$, as a function of the center-of-mass energy for the mass of singlet neutrino N_ℓ equal to 85 GeV and mixing amplitude $|U_\ell| = 0.1$.

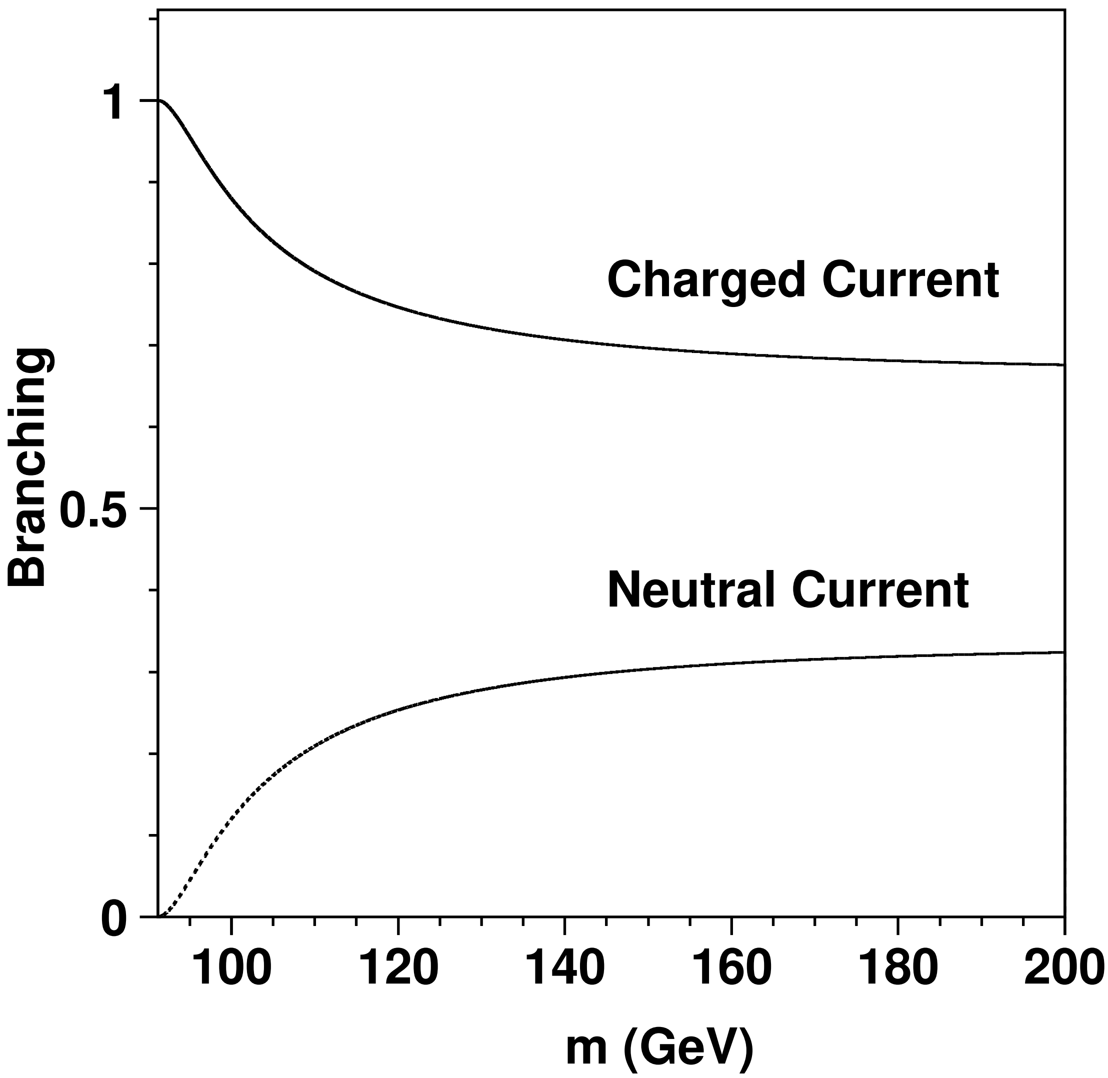

Figure 5: Branching ratios for heavy lepton decays.

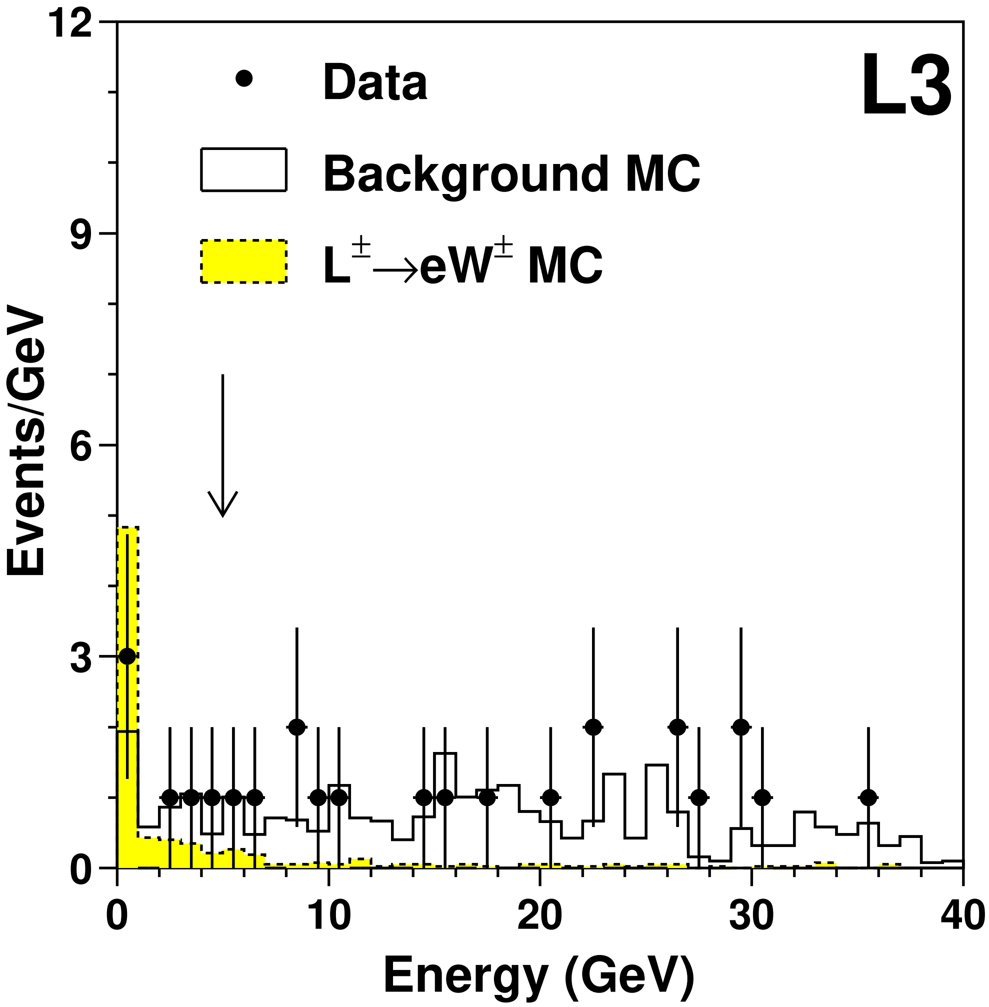

Figure 6: Energy in a 30° cone around the second most energetic electron candidate. The dots are the data, the solid histogram is the background Monte-Carlo. The dashed line represents the simulated signal for $e^+e^- \to L\overline{L}$ from the TIPTOP Monte-Carlo. The normalization for the signal Monte-Carlo is arbitrary. The arrow indicates the corresponding value of the applied cut. In this case, all cuts on other quantities have been applied.

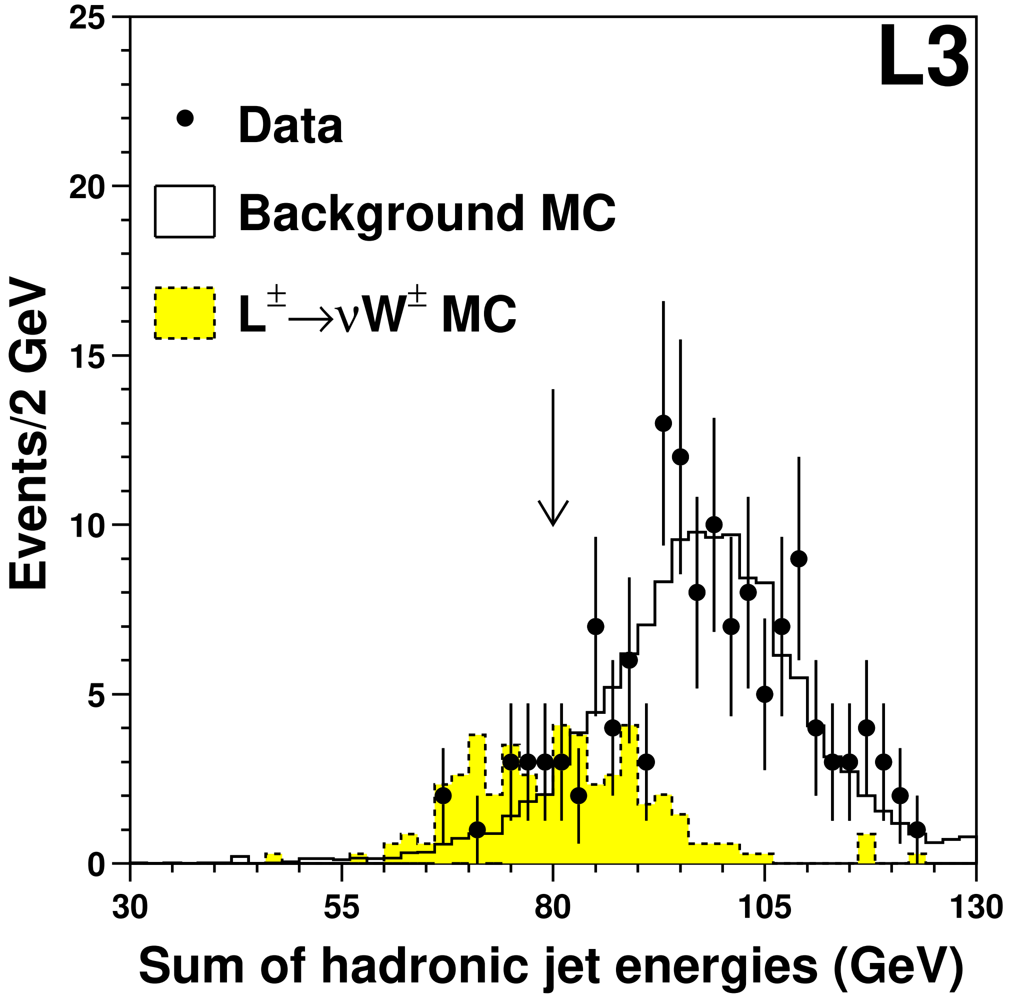

Figure 7: The sum of the energies of the hadronic jets. The dots are the data, the solid histogram is the background Monte-Carlo. The dashed line represents the simulated signal for $e^+e^- \to L\overline{L}$ from the TIPTOP Monte-Carlo. The normalization for the signal Monte-Carlo is arbitrary. The arrow indicates the corresponding value of the applied cut. In this case, all cuts on other quantities have been applied.

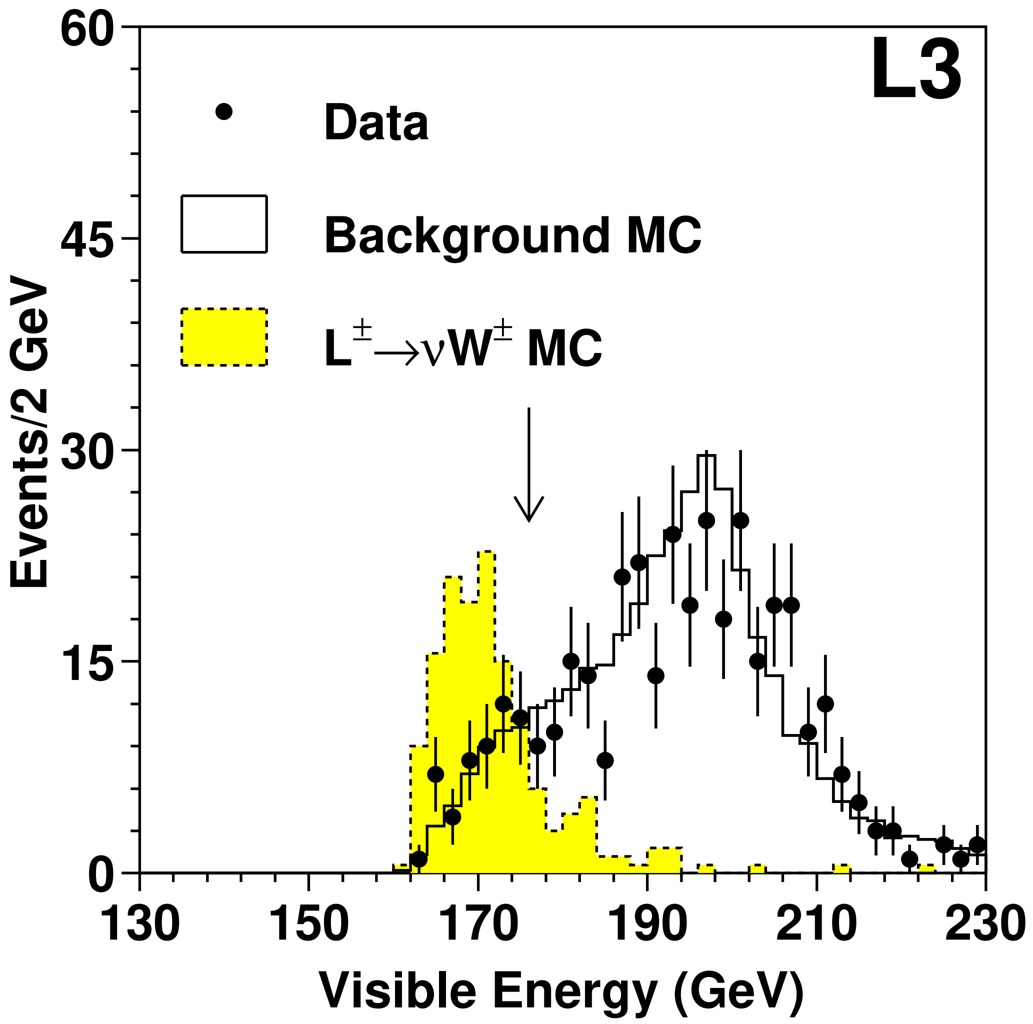

Figure 8: Visible energy in the event. The dots are the data, the solid histogram is the background Monte-Carlo. The dashed line represents the simulated signal for $e^+e^- \rightarrow L\overline{L}$ from the TIPTOP Monte-Carlo. The normalization for the signal Monte-Carlo is arbitrary. The arrow indicates the corresponding value of the applied cut. In this case, all previous cuts on other quantities have been applied.

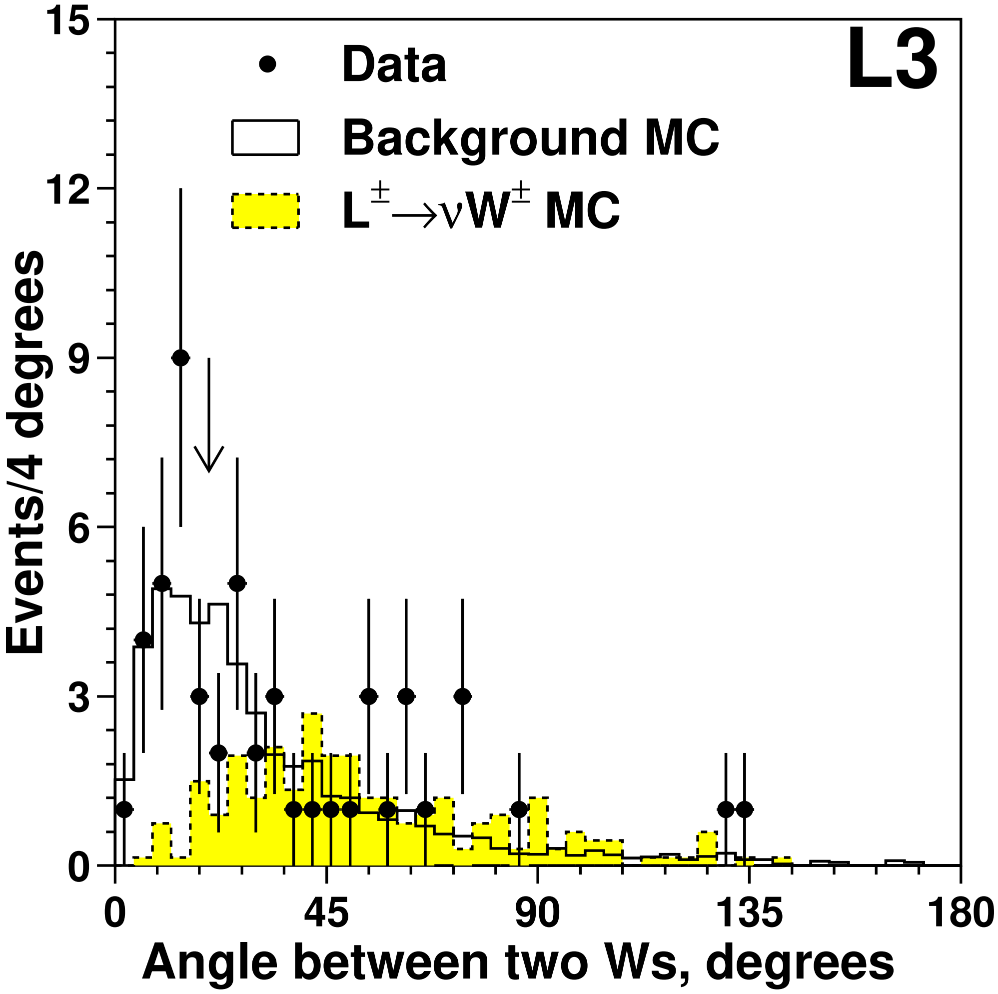

Figure 9: The acollinearity angle between the two W candidates. The dots are the data, the solid histogram is the background Monte-Carlo. The dashed line represents the simulated signal for $e^+e^- \rightarrow L\overline{L}$ from the TIPTOP Monte-Carlo. The normalization for the signal Monte-Carlo is arbitrary. The arrow indicates the corresponding value of the applied cut. In this case, all previous cuts on other quantities have been applied.

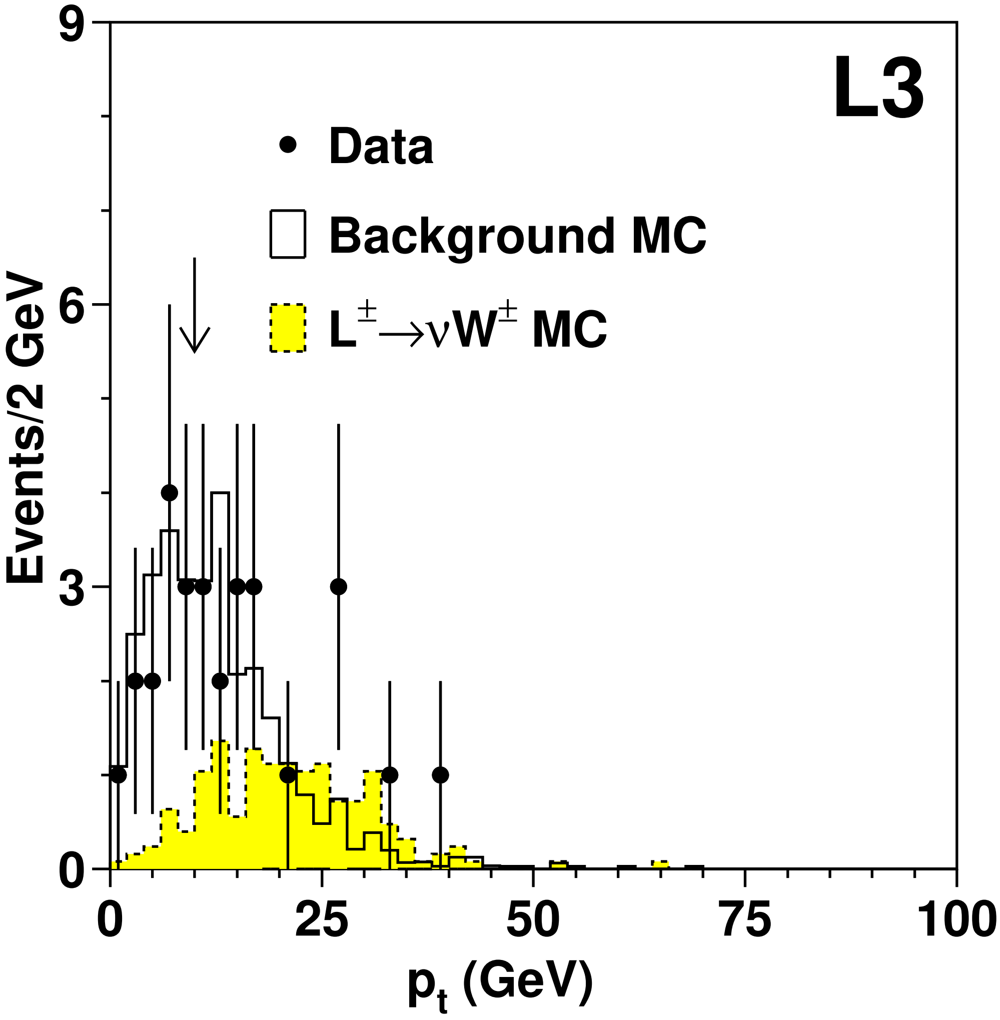

Figure 10: The distribution of the total transverse momentum, p_t. The dots are the data, the solid histogram is the background Monte-Carlo. The dashed line represents the simulated signal for $e^+e^- \to L\overline{L}$ from the TIPTOP Monte-Carlo. The normalization for the signal Monte-Carlo is arbitrary. The arrow indicates the corresponding value of the applied cut. In this case, all cuts on other quantities have been applied.

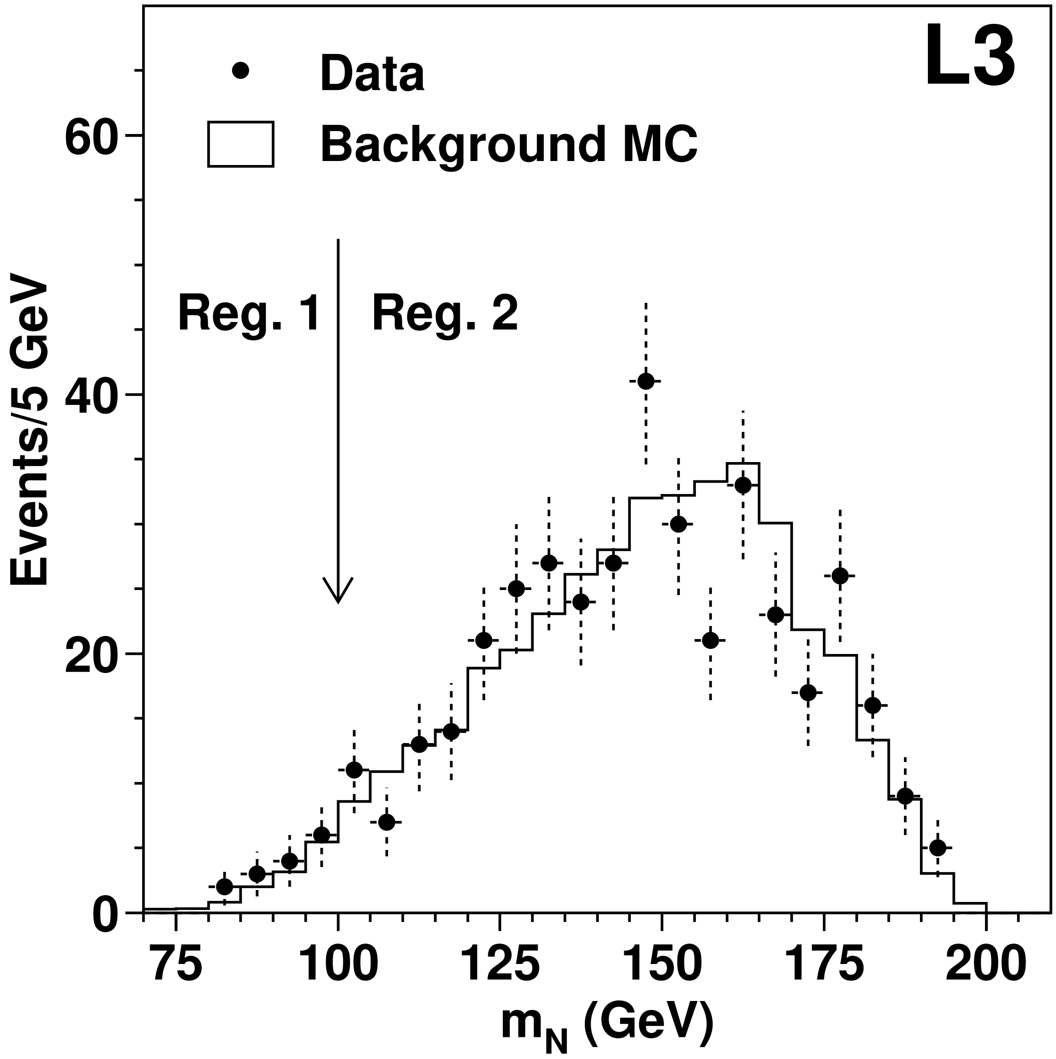

Figure 11: Distribution of the corrected invariant mass of the event. The dots are the data and the solid histogram is the background.

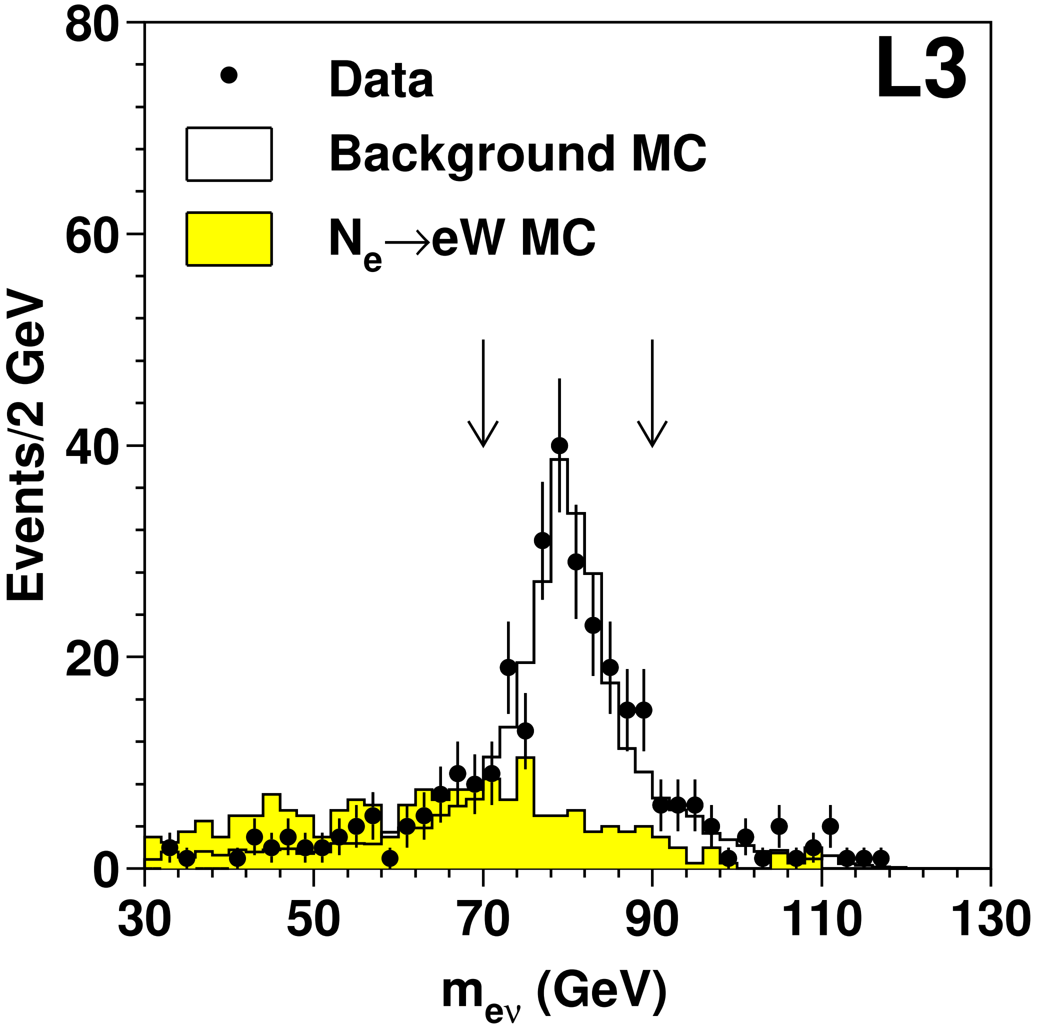

Figure 12: The invariant mass, $m_{e\nu}$, of the isolated lepton and missing momentum. The dots are the data taken at $\sqrt{s}$ = 192−202 GeV, the solid histogram is the background Monte Carlo. The dashed histogram is a predicted signal $e^+e^- \rightarrow \nu N$ for the mass of heavy neutrino $m_N = 155$ GeV. The normalization for the signal Monte Carlo is arbitrary. The arrows indicate the corresponding value of the applied cut.

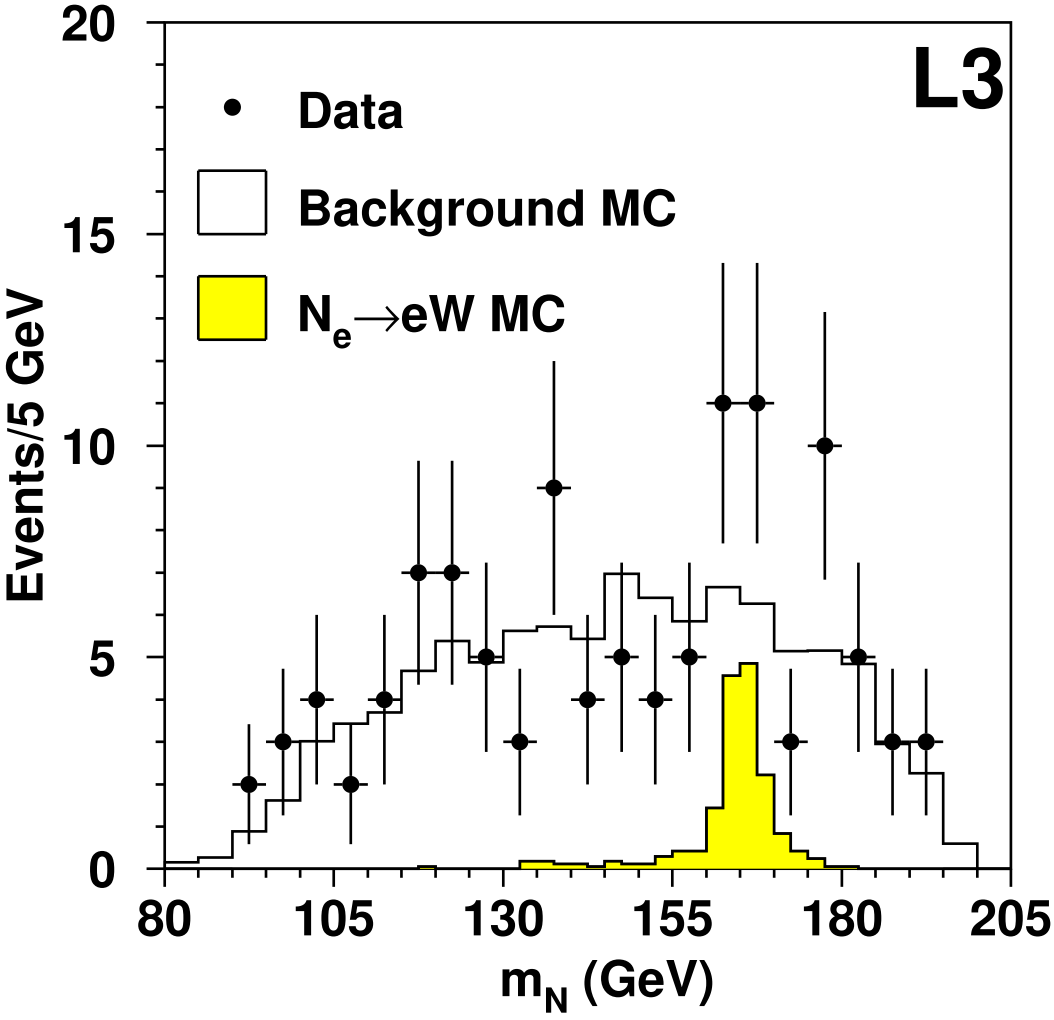

Figure 13: Distribution of the invariant mass of the event after the kinematic fit. The points are the data and the solid histogram is the background MC. The shaded histogram is the predicted signal $e^+e^- \rightarrow \nu N$ for a 165 GeV heavy neutrino. The normalization for the signal Monte Carlo is arbitrary.

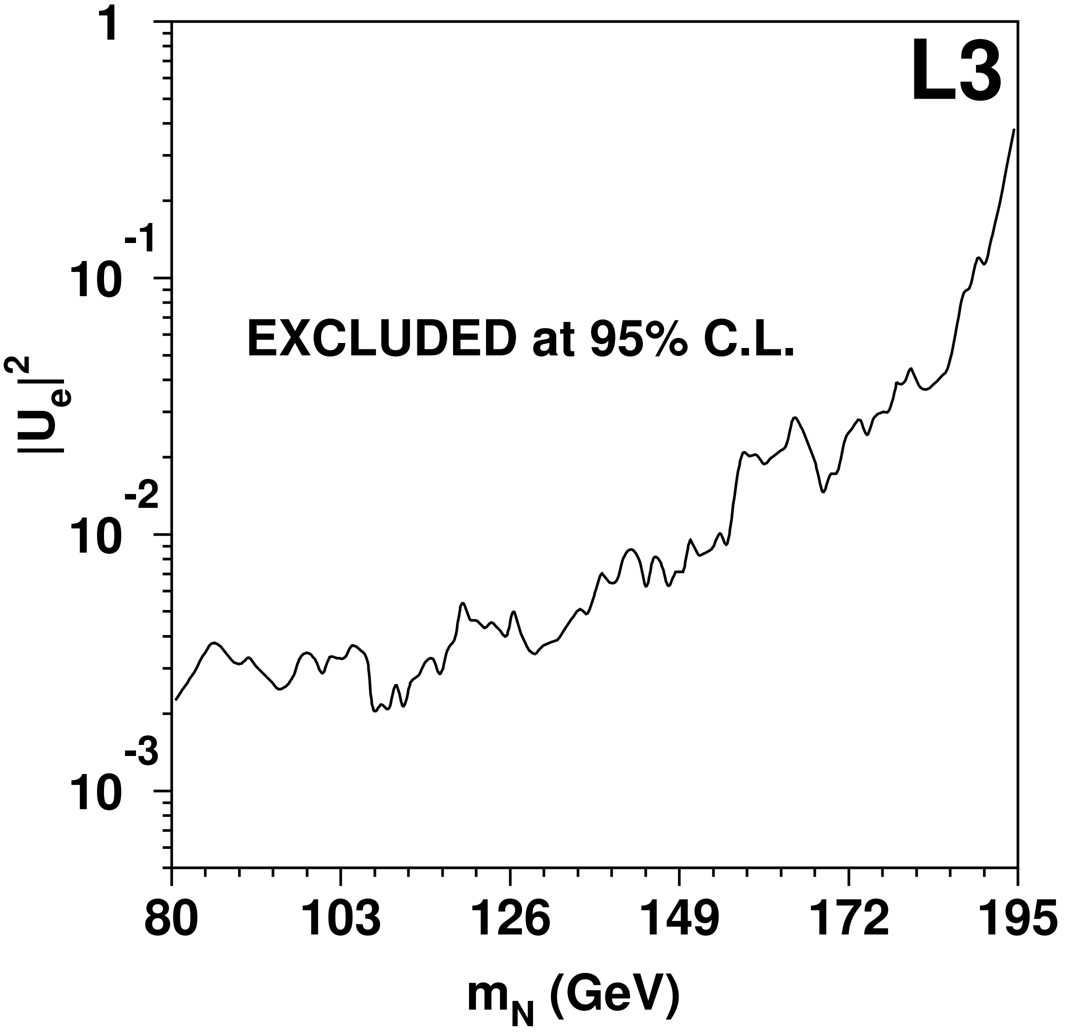

Figure 14: Upper limit at the 95% C.L. on the mixing amplitude as a function of the heavy neutrino mass.